COLD SPRING HARBOR
Molecular Case Studies

RESEARCH REPORT

A novel *PRRT2* pathogenic variant in a family with paroxysmal kinesigenic dyskinesia and benign familial infantile seizures

Jacqueline G. Lu,[1,2] Juliet Bishop,[3] Sarah Cheyette,[4] Igor B. Zhulin,[5,6] Su Guo,[1,7] Nara Sobreira,[3] and Steven E. Brenner[1,8]

[1]Department of Bioengineering and Therapeutic Sciences, University of California, San Francisco, California 94143, USA; [2]Gunn High School, Palo Alto, California 94306, USA; [3]McKusick-Nathans Institute of Genetic Medicine, Johns Hopkins University School of Medicine Baltimore, Maryland 21205, USA; [4]Palo Alto Medical Foundation, Palo Alto, California 94306, USA; [5]Computational Sciences and Engineering Division, Oak Ridge National Laboratory, Oak Ridge, Tennessee 37831, USA; [6]Department of Microbiology, University of Tennessee, Knoxville, Tennessee 37914, USA; [7]Institute for Human Genetics and Programs in Biological Sciences, University of California, San Francisco, California 94143, USA; [8]Department of Computational Biology, University of California, Berkeley, California 94720, USA

Abstract Paroxysmal kinesigenic dyskinesia (PKD) is a rare neurological disorder characterized by recurrent attacks of dyskinetic movements without alteration of consciousness that are often triggered by the initiation of voluntary movements. Whole-exome sequencing has revealed a cluster of pathogenic variants in *PRRT2* (proline-rich transmembrane protein), a gene with a function in synaptic regulation that remains poorly understood. Here, we report the discovery of a novel *PRRT2* pathogenic variant inherited in an autosomal dominant pattern in a family with PKD and benign familial infantile seizures (BFIS). After targeted Sanger sequencing did not identify the presence of previously described *PRRT2* pathogenic variants, we carried out whole-exome sequencing in the proband and her affected paternal grandfather. This led to the discovery of a novel *PRRT2* variant, NM_001256442:exon3:c.C959T/NP_660282.2:p.A320V, altering an evolutionarily conserved alanine at the amino acid position 320 located in the M2 transmembrane region. Sanger sequencing further confirmed the presence of this variant in four affected family members (paternal grandfather, father, brother, and proband) and its absence in two unaffected ones (paternal grandmother and mother). This newly found variant further reinforces the importance of *PRRT2* in PKD, BFIS, and possibly other movement disorders. Future functional studies using animal models and human pluripotent stem cell models will provide new insights into the role of *PRRT2* and the significance of this variant in regulating neural development and/or function.

Corresponding authors:
jackielu812@gmail.com;
su.guo@ucsf.edu

Ontology terms: ataxia; autism; extrapyramidal dyskinesia; focal autonomic seizures without altered responsiveness; infantile spasms; intellectual disability, profound; migraine without aura; paroxysmal dyskinesia

Published by Cold Spring Harbor Laboratory Press

doi: 10.1101/mcs.a002287

[Supplemental material is available for this article.]

INTRODUCTION

Paroxysmal kinesigenic dyskinesia (PKD; OMIM 128200) is a rare neurological disorder with around 1500 cases reported thus far, affecting approximately 1 in 150,000. The disease is characterized by a series of involuntary and uncontrollable motor activities whenever the affected individual attempts to initiate movements after a period of being static (Nobile and Striano 2014; Ebrahimi-Fakhari et al. 2015; Valtorta et al. 2016). Previous studies have linked this disease to the *PRRT2* (proline-rich transmembrane protein) gene (Chen et al. 2011; Lee et al.

2012), which is reportedly responsible for a multitude of neurological disorders including not only PKD but also benign familial infantile seizures (BFIS; OMIM 605751), which occurs in infancy with onset between 3 and 12 mo of age and is characterized by brief seizures with motor arrest, cyanosis, hypertonia, and limb jerks. Seizures respond well to antiepileptic drugs and usually remit around 2 yr of age (Callenbach et al. 2002). Additional conditions include infantile convulsions and choreoathetosis (ICCA; OMIM 602066) and, in severe cases, intellectual disability (ID) (Nobile and Striano 2014; Ebrahimi-Fakhari et al. 2015; Valtorta et al. 2016).

Consisting of four exons, the *PRRT2* gene resides on Chromosome 16p11.2. Loss-of-function heterozygous *PRRT2* variants have been found in ~85%–90% of familial cases of PKD, BFIS, and ICCA. The most common variant identified is the frameshift single-nucleotide duplication NM_001256442:c.649dupC (p.R217fsX224), which was found in 62% of PKD, ICCA, and BFIS families. Moreover, homozygous *PRRT2* variants have been linked to intellectual disability, emphasizing the importance of the gene in brain development and/or function. In sporadic cases, many fewer (34% of families) were discovered to have *PRRT2* variants, suggesting either the involvement of other genes or the existence of undiscovered variants on the *PRRT2* gene (Nobile and Striano 2014).

Here we report the identification of a novel pathogenic variant in a family with PKD and BFIS that is inherited in an autosomal dominant pattern. Targeted sequencing did not identify the presence of previously described *PRRT2* variants in the family. Subsequent whole-exome sequencing (WES) uncovered a novel variant at the amino acid position 320, which changed alanine to valine. Sanger sequencing further verified the presence of this variant in all affected family members and its absence in the unaffected ones. A320 is located in the carboxy-terminal transmembrane domain, and its evolutionary conservation suggests functional importance.

RESULTS

Clinical Presentation and Family History

The proband (Individual III-1)'s symptoms started at age 9 1/2, with cramps in both arms and legs. It was noted that sudden movement triggers symptoms, such as standing up after a long sitting period or a rapid transition from standstill to running or even walking. Cramping lasted 15–20 sec. There was no weakness or numbness. Frequencies were irregular. Since onset, the proband has been stable and is not on medication.

Similar symptoms were present in the father of the proband (II-1) (Fig. 1B), who presented at a similar age. His symptoms gradually disappeared in his 20s. He was never treated. His younger brother (II-5) also had similar cramping symptoms. Family history was also notable for seizures, thought to be BFIS. Seizures were present in the proband's brother (III-2), paternal grandfather (I-1), and a paternal uncle (II-3) all of whom outgrew seizures by ages 2–3, and all of whom have had a normal development without muscle cramping. Together, there was a strong family history of both PKD and BFIS.

Genomic Analysis

Given the prevalence of PRRT2 variants in PKD and BFIS, we first used Sanger sequencing to search for possible *PRRT2* variants in the proband (Fig. 2A,B). The two previously described pathogenic variants, *c.649dupc* and *c.133-136delCCAG*, were not detected (Fig. 2C). Although several synonymous changes were discovered, no other variants were uncovered that might account for the disease phenotypes.

We next carried out WES of the proband (III-1) and her affected paternal grandfather (I-1) (Table 1). This approach identified the following rare heterozygous variant: NM_001256442: exon3:c.C959T (NP_660282.2:p.A320V), in exon 3 of *PRRT2*. We further validated this

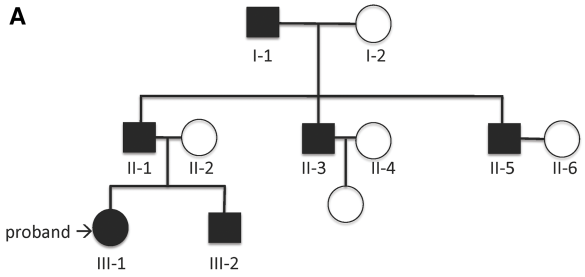

B

Affected individuals	Clinical phenotypes
I-1	PKD, BFIS
II-1	PKD
II-3	BFIS
II-5	PKD
III-1	PKD
III-2	BFIS, PKD unknown

Figure 1. Pedigree of the affected family indicates a dominant inheritance pattern with distinct clinical phenotypes. (*A*) Pedigree with individuals numbered. (*B*) Affected individuals with their known clinical phenotypic manifestations. At the time of this study, III-2 has not reached the age for the manifestation of PKD.

variant by Sanger sequencing. All affected family members carried the variant in heterozygous states, whereas unaffected family members did not have the variant (Fig. 3). Thus, the segregation of the variant with the phenotype in this family was confirmed.

We also revisited the previous Sanger sequencing data of the proband. Manual evaluation of the sequence chromatograms detected a large peak of C and a small peak that represented T in the nucleotide position 959, but the base-calling program Phred failed to make a call for the variant.

The c.C959T (p.A320V) variant is novel and has not been reported in the 1000 Genomes Project (2577 samples, build 20130502, accessed November 2015), dbSNP build 131,

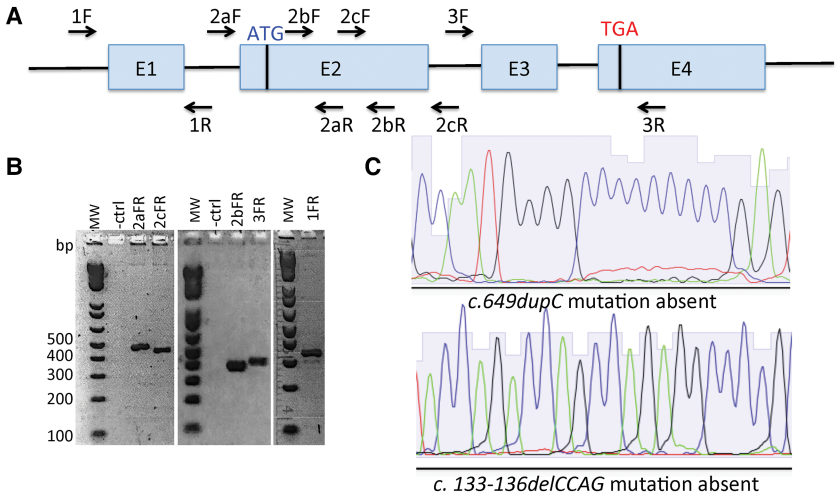

Figure 2. Sanger sequencing of the *PRRT2* gene in the proband excludes the presence of common variants. (*A*) *PRRT2* gene structure with exons/introns demarcated. Locations of the PCR primers are indicated. (*B*) Gel electrophoresis images show the PCR products amplified from the proband genomic DNA with various pairs of primers. (*C*) Representative traces from Sanger sequencing show the absence of two commonly detected *PRRT2* variants in the proband.

Table 1. *PRRT2* (*NG_032039.1*)

Chr: position GRCh37 (hg19)	HGVS	Gene coverage	Variant read depth	Variant type	Predicted effect (SIFT/ PolyPhen)	Population database MAF	Genotype	ClinVar ID
16: 29825733	NM_001256442: exon3: c.C959T NP_660282.2: p.A320V	100% at 20×	65	Missense	Deleterious/ probably damaging	None reported	Heterozygous	SCV000606838

HGVS, Human Genome Variation Society; MAF, mean allele frequency in 1000 Genomes, dbSNP build 131, and ExAC databases.

Exome Variant Server release ESP6500SI-V2 (6503 samples, accessed November 2015), or Exome Aggregation Consortium (ExAC) database (60,706 samples, accessed November 2015). It has a Combined Annotation Dependent Depletion (CADD) (Kircher et al. 2014) score of 20.9, which is in the top 1% of all ~8.7 billion possible single-nucleotide variants (SNVs) in terms of predicted deleteriousness. *PRRT2* variants are known to cause phenotypes consistent with those observed in this family.

To shed light on the potential functional significance of this variant, we examined the position A320 relative to the overall topology of the PRRT2 protein. Based on a previously reported structural model generated with the Rosetta structure prediction software suite and molecular dynamics simulation, we found that p.A320 was located in the carboxy-terminal transmembrane domain (Fig. 4A), which is the most conserved part of the protein. We used an evolutionary approach, termed SAVER, to predict disease-causing single amino acid substitutions (Adebali et al. 2016), by including orthologous, but not paralogous,

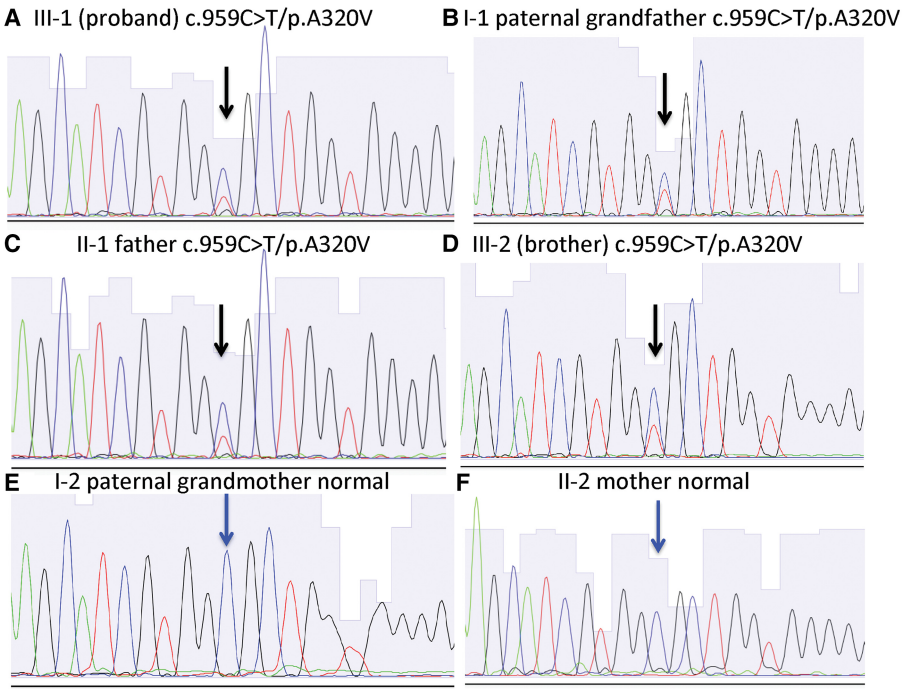

Figure 3. Segregation of a novel pathogenic *PRRT2* variant uncovered via whole-exome sequencing with phenotypic characteristics of PKD and BFIS. Representative traces from Sanger sequencing show the 100% concordance of the c.959C>T/p.A320V variant with the affected individuals in the family.

sequences into consideration. The *PRRT2* gene was duplicated in a common ancestor of bony fishes (Supplemental Fig. S1), and all PRRT2 orthologs in vertebrates contain alanine in position 320 (Fig. 4B,C; Supplemental Fig. S2), except for bony fishes. The bony fish *PRRT2* orthologs contain serine in this position. Consequently, any substitution of A320, other than serine, in the human PRRT2 is predicted to be damaging. Together, these observations suggest that the newly discovered A320V variant is disease-causing.

DISCUSSION

Here we report the finding of a novel pathogenic variant p.A320V in the *PRRT2* gene that is linked to a rare familial neurological disorder, with multifaceted phenotypic presentations including PKD and BFIS. The alanine 320 is conserved in PRRT2 orthologs from all vertebrates examined including the primitive lungfish, with the exception of bony fishes, where the duplication of the *PRRT2* gene and the A320S substitution was detected, which is consistent with the fact that this clade undergoes rapid genomic evolution (Brazeau and Friedman

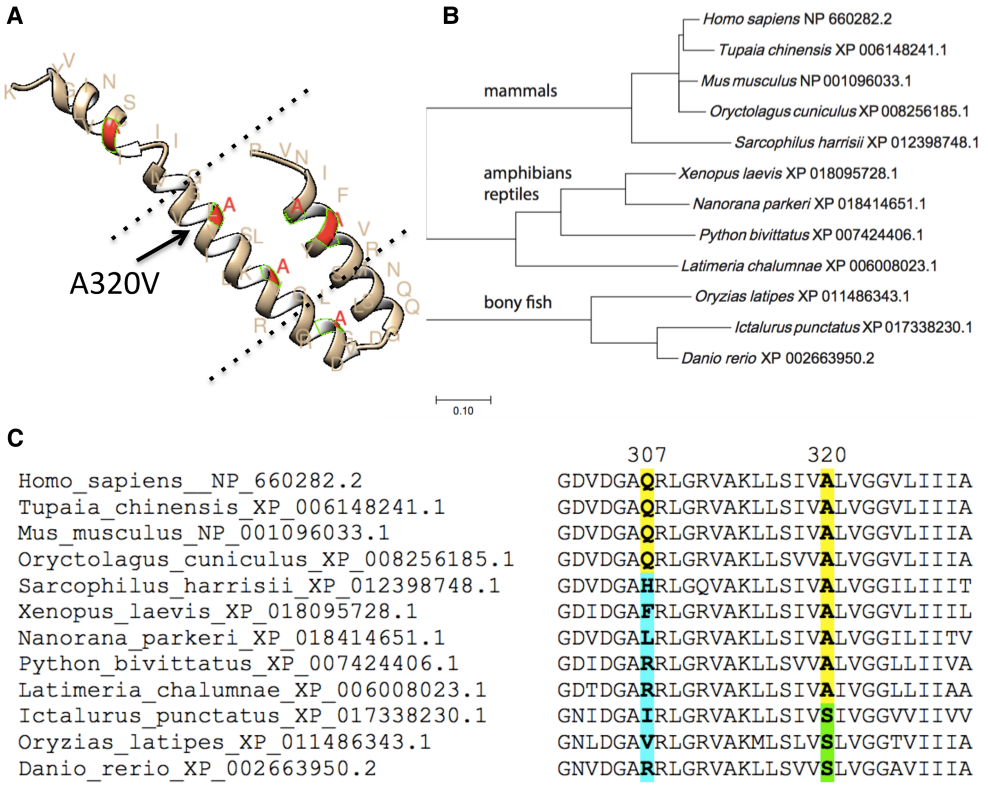

Figure 4. The location of alanine 320 in the PRRT2 protein and its evolutionary conservation. (*A*) A structural model of the PRRT2 protein transmembrane domains (residues 261–340). The protein backbone is shown as a schematic, with alanine residues colored in red. Dashed lines indicate putative membrane limits. The structural model was from Rossi et al. (2016). (*B*) Maximum likelihood phylogenic tree of the representative PRRT2 orthologs across vertebrates. The tree is drawn to scale, with branch lengths measured in the number of substitutions per site. All positions containing gaps were eliminated; there were a total of 146 positions in the final data set. (*C*) Multiple protein sequence alignment of the PRRT2 sequence region encompassing the A320 residue in representative vertebrate species. Conserved Ala in position 320 is highlighted in yellow, and Ser, which is conserved in this position in bony fishes, is highlighted in green. Substitutions in position 307 are highlighted in blue. An alignment of this region in all detected PPR2 homologs is shown in Supplemental Figure S2.

2015). It is also of interest to note that the *PRRT2* gene is completely missing from birds, whereas it is present in earlier branches of life. This might highlight some unique features of the avian brain, which make the *PRRT2* gene function dispensable.

A twist in the discovery of this novel pathogenic variant is worth noting. Given the clear role of *PRRT2* in PKD, the Sanger sequencing method was initially used to sequence this gene in the proband in our academic laboratory. However, the variant was not called through a standard base-calling method such as Phred. Remarkably, it was through the WES that this variant was discovered, which was subsequently confirmed by Sanger sequencing. The initial miss was due to sole reliance on the base-calling program. Going forward, it is important to use orthogonal techniques when examining a strong candidate gene suspected to be involved in patients under study. Other base-calling programs such as Mutation Surveyor can be used to better identify heterozygous variants. It is also critical to manually review sequence chromatograms that may contain "double" peaks. Our study exemplifies the power of exome sequencing to identify variants that could be missed by Sanger sequencing.

The *PRRT2* gene is located in an important CNV (copy-number variation) region, 16p11.2. Microduplications of 16p11.2 are associated with schizophrenia (McCarthy et al. 2009), whereas its microdeletion is associated with aortic valve development, seizure disorder, and mental retardation (Ghebranious et al. 2007). In addition to PKD and BFIS found in the family of this study, *PRRT2* variants are also involved in other conditions such as migraine, hemiplegic migraine, episodic ataxia, and intellectual disability (Nobile and Striano 2014; Ebrahimi-Fakhari et al. 2015). A recent case report of benign infantile seizures followed by autistic regression in a boy with 16p11.2 deletion further highlights the importance of PRRT2 in human brain development (Milone et al. 2017). Despite its importance in human clinical phenotypes, the biological function of PRRT2 remains poorly understood. Recent studies using cultured primary mouse neurons show that the protein is enriched in presynaptic terminals and plays a critical role in maintaining synaptic numbers and baseline docked synaptic vesicles at rest. PRRT2-deficient neurons show marked impairment in synchronous release as a result of a significant decrease in release probability and Ca^{2+} sensitivity (Valente et al. 2016; Valtorta et al. 2016). PRRT2 knockout mice have been generated, which show paroxysmal movements resembling human conditions (Michetti et al. 2017). Future studies utilizing animal models and human pluripotent stem cell–derived neurons shall further address how PRRT2 may interact with other synaptic proteins such as SNAP-25 and synaptotagmin 1/2 to regulate neural circuit dynamics and function.

METHODS

Sample Collection, PCR, and Sanger Sequencing

Saliva samples were collected from individual members of the family for genomic DNA extraction using a kit (OGR-500, Cat# PD-LB-00191, DNA Genotek Inc.). PCR primers were designed according to previously published sequences (Chen 2015) and used to amplify genomic fragments. PCR products were subjected to Sanger sequencing (Quintara Biosciences, Inc., SimpliSeq DNA Sequencing) (Table 2). In brief, PCR products were mixed with one of the PCR primers (serving as the sequencing primer), DNA polymerase, standard deoxynucleotides, and one of the four dideoxynucleotides (ddATP, ddGTP, ddCTP, or ddTTP).

WES and Variant Analysis

We performed WES in the proband and her affected paternal grandfather. The CCDS exonic regions and flanking intronic regions totaling ~51 Mb were captured using the Agilent

Table 2. Sequencing results

Patient	Total reads	Total mapped reads	Filtered variants	Yield (Gb)	Mean target coverage	Mean target coverage >20× (%)	>Q30 (%)	Mean Q
III-1	71947232	66390616	138584	6.62	72.1	93.1	94.3	36
I-1	68909304	62494642	138460	6.23	66.8	91.7	94.3	36

SureSelect XT kit and we performed paired-end 100-bp reads with the Illumina HiSeq2500 platform. Each read was aligned to the 1000 Genomes phase 2 (GRCh37) human genome reference with the Burrows–Wheeler Alignment v.0.5.10-tpx (Li and Durbin 2009). Local realignment around indels and base call quality score recalibration were performed with the Genome Analysis Toolkit (GATK) (McKenna et al. 2010) v.2.3-9-ge5ebf34. Variant filtering was done via the Variant Quality Score Recalibration (VQSR) method (DePristo et al. 2011). For SNVs, the annotations of MQRankSum, HaplotypeScore, QD, FS, MQ, and ReadPosRankSum were used in the adaptive error model (6 max Gaussians allowed; worst 3% used for training the negative model). HapMap3.331 and Omni2.5 were used as training sites with HapMap3.3 used as the truth set. SNVs were filtered to obtain all variants up to the 99th percentile of truth sites (1% false negative rate). For indels, the annotations of QD, FS, HaplotypeScore, and ReadPosRankSum were used in the adaptive error model (4 max Gaussians allowed; worst 12% used for training the negative model; indels that had annotations of >10 SD from the mean were excluded from the Gaussian mixture model). A set of curated indels obtained from the GATK resource bundle (Mills_and_1000G_gold_ standard.indels.b37.vcf) were used as training and truth sites. Indels were filtered to obtain all variants up to the 95th percentile of truth sites (5% false negative rate). Using the PhenoDB Variant Analysis Tool of PhenoDB, we prioritized heterozygous, homozygous, and compound heterozygous rare functional variants (missense, nonsense, splice site variants, and indels) shared by the proband and her paternal grandfather. The variants were furthered filtered using OMIM phenotypes that matched the phenotypic features of the proband and paternal grandfather entered into PhenoDB (Sobreira et al. 2015). We excluded variants with a minor allele frequency (MAF) of >0.01 in dbSNP 126, 129, and 131, the Exome Variant Server (release ESP6500SI-V2), 1000 Genomes Project or among the samples sequenced at CIDR as part of the BHCMG. Only the reported variant in the *PRRT2* gene was uncovered.

Evolutionary Sequence Analysis

Orthologs of the human PRRT2 protein were identified by BLAST searches against the NCBI RefSeq database, followed by a multiple sequence alignment and construction of the maximum likelihood phylogenetic tree using MEGA7 (Kumar et al. 2016). Gene duplication events were inferred from the tree topology and paralogous sequences were excluded from further analysis. Conservation of individual amino acid positions was assessed using a custom consensus script.

ADDITIONAL INFORMATION

Data Deposition and Access

The sequence data for the two individuals whose DNA underwent exome sequencing (III-1 [BH8378_1] and I-1 [BH8378_8]) were submitted to dbGaP with a submission number phs000711.v5.p2. The *PRRT2* variant has been submitted to ClinVar (http://www.ncbi.nlm.nih.gov/ clinvar/) under accession number SCV000606838.

Ethics Statement

Written informed consent was obtained from all study participants in accordance with approved protocols from the Institutional Review Board of the Johns Hopkins University and the University of California, San Francisco.

Acknowledgments

We are indebted to the family described in the manuscript for their participation in the study. We thank Drs. Luca Maragliano and Fabio Benfenati at the Center for Synaptic Neuroscience and Technology, Italy for sharing the molecular dynamics simulation file of the PRRT2 carboxy-terminal region, Drs. Elaine Meng and Thomas Ferrin at UCSF for discussions on interpreting the molecular dynamics simulation data, and Dr. Dane Witmer for his assistance in locating information related to the WES analysis.

Author Contributions

J.G.L., S.G., and S.E.B. conceived and designed the experiments. J.G.L. performed DNA preparation, PCR, and variant validation through Sanger sequencing analysis. J.B. and N.S. performed the exome sequencing and data analysis. S.C. provided the clinical analysis. I.B.Z. performed evolutionary sequence analysis. J.G.L. drafted the manuscript with all authors' inputs.

Competing Interest Statement

The authors have declared no competing interest.

Received August 13, 2017; accepted in revised form November 2, 2017.

Funding

This research was supported by the following funding sources from the National Institutes of Health: R01 GM072285 (I.B.Z.), R01 NS095734 (S.G.), R01 AI105776 (S.E.B.), U41 HG007346 (S.E.B.), 1U54 HG006542 (N.S.), and Tata Consultancy Services (S.E.B.).

REFERENCES

Adebali O, Reznik AO, Ory DS, Zhulin IB. 2016. Establishing the precise evolutionary history of a gene improves prediction of disease-causing missense mutations. *Genet Med* **18:** 1029–1036.

Brazeau MD, Friedman M. 2015. The origin and early phylogenetic history of jawed vertebrates. *Nature* **520:** 490–497.

Callenbach PM, de Coo RF, Vein AA, Arts WF, Oosterwijk J, Hageman G, ten Houten R, Terwindt GM, Lindhout D, Frants RR, et al. 2002. Benign familial infantile convulsions: a clinical study of seven Dutch families. *Eur J Paediatr Neurol* **6:** 269–283.

Chen GH. 2015. Five cases of paroxysmal kinesigenic dyskinesia by genetic diagnosis. *Exp Ther Med* **9:** 909–912.

Chen WJ, Lin Y, Xiong ZQ, Wei W, Ni W, Tan GH, Guo SL, He J, Chen YF, Zhang QJ, et al. 2011. Exome sequencing identifies truncating mutations in *PRRT2* that cause paroxysmal kinesigenic dyskinesia. *Nat Genet* **43:** 1252–1255.

DePristo MA, Banks E, Poplin R, Garimella KV, Maguire JR, Hartl C, Philippakis AA, del Angel G, Rivas MA, Hanna M, et al. 2011. A framework for variation discovery and genotyping using next-generation DNA sequencing data. *Nat Genet* **43:** 491–498.

Ebrahimi-Fakhari D, Saffari A, Westenberger A, Klein C. 2015. The evolving spectrum of *PRRT2*-associated paroxysmal diseases. *Brain* **138:** 3476–3495.

Ghebranious N, Giampietro PF, Wesbrook FP, Rezkalla SH. 2007. A novel microdeletion at 16p11.2 harbors candidate genes for aortic valve development, seizure disorder, and mild mental retardation. *Am J Med Genet A* **143A:** 1462–1471.

Kircher M, Witten DM, Jain P, O'Roak BJ, Cooper GM, Shendure J. 2014. A general framework for estimating the relative pathogenicity of human genetic variants. *Nat Genet* **46:** 310–315.

Kumar S, Stecher G, Tamura K. 2016. MEGA7: Molecular Evolutionary Genetics Analysis Version 7.0 for bigger datasets. *Mol Biol Evol* **33:** 1870–1874.

Lee HY, Huang Y, Bruneau N, Roll P, Roberson ED, Hermann M, Quinn E, Maas J, Edwards R, Ashizawa T, et al. 2012. Mutations in the gene *PRRT2* cause paroxysmal kinesigenic dyskinesia with infantile convulsions. *Cell Rep* **1:** 2–12.

Li H, Durbin R. 2009. Fast and accurate short read alignment with Burrows–Wheeler transform. *Bioinformatics* **25:** 1754–1760.

McCarthy SE, Makarov V, Kirov G, Addington AM, McClellan J, Yoon S, Perkins DO, Dickel DE, Kusenda M, Krastoshevsky O, et al. 2009. Microduplications of 16p11.2 are associated with schizophrenia. *Nat Genet* **41:** 1223–1227.

McKenna A, Hanna M, Banks E, Sivachenko A, Cibulskis K, Kernytsky A, Garimella K, Altshuler D, Gabriel S, Daly M, et al. 2010. The Genome Analysis Toolkit: a MapReduce framework for analyzing next-generation DNA sequencing data. *Genome Res* **20:** 1297–1303.

Michetti C, Castroflorio E, Marchionni I, Forte N, Sterlini B, Binda F, Fruscione F, Baldelli P, Valtorta F, Zara F, et al. 2017. The *PRRT2* knockout mouse recapitulates the neurological diseases associated with *PRRT2* mutations. *Neurobiol Dis* **99:** 66–83.

Milone R, Valetto A, Bertini V, Sicca F. 2017. Benign infantile seizures followed by autistic regression in a boy with 16p11.2 deletion. *Epileptic Disord* **19:** 222–225.

Nobile C, Striano P. 2014. PRRT2: a major cause of infantile epilepsy and other paroxysmal disorders of childhood. *Prog Brain Res* **213:** 141–158.

Rossi P, Sterlini B, Castroflorio E, Marte A, Onofri F, Valtorta F, Maragliano L, Corradi A, Benfenati F. 2016. A Novel Topology of Proline-Rich Transmembrane Protein 2 (PRRT2): hints for an intracellular function at the synapse. *J Biol Chem* **291:** 6111–6123.

Sobreira N, Schiettecatte F, Boehm C, Valle D, Hamosh A. 2015. New tools for Mendelian disease gene identification: PhenoDB variant analysis module; and GeneMatcher, a web-based tool for linking investigators with an interest in the same gene. *Hum Mutat* **36:** 425–431.

Valente P, Castroflorio E, Rossi P, Fadda M, Sterlini B, Cervigni RI, Prestigio C, Giovedì S, Onofri F, Mura E, et al. 2016. PRRT2 is a key component of the Ca^{2+}-dependent neurotransmitter release machinery. *Cell Rep* **15:** 117–131.

Valtorta F, Benfenati F, Zara F, Meldolesi J. 2016. PRRT2: from paroxysmal disorders to regulation of synaptic function. *Trends Neurosci* **39:** 668–679.